Available online at www.sciencedirect.com
SCIENCE DIRECT
Physics Letters A 350 (2006) 283–287
PHYSICS LETTERS A
www.elsevier.com/locate/pla

Resistivity properties of the mixed-phase manganite $La_{0.96}Te_{0.04}MnO_3$

Qing-li Zhou, Kui-juan Jin *, Dong-yi Guan, Zheng-hao Chen, Hui-bin Lu, Guo-zhen Yang

Beijing National Laboratory for Condensed Matter Physics, Institute of Physics, Chinese Academy of Sciences, P.O. Box 603, Beijing 100080, China

Received 17 June 2005; accepted 26 September 2005

Available online 18 October 2005

Communicated by J. Flouquet

Abstract

Based on the phase separation scenario, the resistivity of $La_{0.96}Te_{0.04}MnO_3$ is investigated by using the random network model. The good quantitative simulated results reveal that the magnetic field-induced change results in the resistivity reduction and the colossal magnetoresistance. Assuming a thermal hysteresis of magnetization, our approach yields a reasonable prediction of thermal hysteresis of resistivity.

PACS: 75.47.Lx; 64.75.+g; 84.37.+q

Keywords: Manganite; Phase separation; Resistivity

1. Introduction

Manganites $A_{1-x}B_xMnO_3$ (where A = rare earth cation and B = divalent or tetravalent cation) have attracted much attention since the observation of the colossal magnetoresistance (CMR) effect and the related physical properties. Experimentally, those manganites usually exhibit a metal-to-insulator transition (MIT) accompanied by a simultaneous phase-to-phase transition near the Curie temperature T_c, such as ferromagnetic (FM) metallic to paramagnetic (PM) insulating transition in $(La_{1-x}Te_x)_{2/3}Ca_{1/3}MnO_3$ [1], $(La_{1-x}Y_x)_{2/3}Ca_{1/3}MnO_3$ and $La_{1-x}Te_xMnO_3$ [2,3], or FM to charge ordering transition in $La_{0.5}Ca_{0.5}MnO_3$ [4], $(La_{1-x}Pr_x)_{5/8}Ca_{3/8}MnO_3$ [5] and $Pr_{1-x}Ca_xMnO_3$ [6]. Furthermore, when applying a magnetic field, the temperature of MIT moves to a higher value and the resistivity decreases correspondingly. Theoretically, the early work focused on the qualitative explanation of the transport and magnetic properties, such as the double exchange model (DE) [7]. Accumulating evidence indicates that one of the important features of the manganites is the competition between double-exchange ferromagnetism and another instability associated with electron–lattice coupling [8]. In addition, magnetic polarons [9], spin-polarons [10], and orbital ordering effects [11] have been considered to explain the observed physical properties. However, they are not sufficient in explaining the phase transition and the enormous magnitude of magnetoresistance [12].

A promising description is the percolative conduction in the mixed-phase state. It suggests that the manganites have strong tendency toward phase separation with intrinsic inhomogeneity. Rodriguez-Martinez et al. [13] have shown that the disorder introduced by chemical replacements in the A-sites is also significant in determining the properties of manganite oxides. Moreover, the experimental results showing the coexisting clusters in $(La_{1-x}Pr_x)_{5/8}Ca_{3/8}MnO_3$ indicate intrinsic inhomogeneities in the system [4]. Fäth et al. [14] have observed the coexistence of PM and FM regions below T_c by the scanning tunneling spectroscopy. Based on the mixed-phase scenario, Mayr et al. [5] simulated the resistivity of temperature dependence and obtained a qualitative agreement with some experiments.

In this Letter, by introducing the breadth-first traversal (BFT) algorithm, we present a calculation method for the random network model to simulate the conductive behavior based on the phase-separated framework for $La_{0.96}Te_{0.04}MnO_3$ (LTMO). The empirical formulas are proposed for resistivities

* Corresponding author. Tel. and fax: +86 10 82648099.
E-mail address: kjjin@aphy.iphy.ac.cn (K.-j. Jin).

0375-9601/$ – see front matter
doi:10.1016/j.physleta.2005.09.079

in the FM and PM domains as functions of temperature T, including the magnetic scattering effect. The theoretical results give good agreement with our experimental data, showing MITs in the temperature range from 5 K to 300 K under the zero or nonzero external magnetic fields. We found that the external magnetic field H can suppress electron–electron scattering and magnon scattering, reduce the activation energy, and slightly increase the FM metallic volume, inducing the resistivity reduction and the CMR phenomenon. This finding is the first time to be proved for LTMO material by simulation. By assuming the thermal hysteresis effect of the magnetization in such materials, a similar phenomenon of resistivity is obtained in the thermal cycle. The studies indicate the coexistence of the phases is crucial for understanding the physics of manganites.

2. Model and method

A schematic representation of the percolative framework is presented in Fig. 1. Two-dimensional (2D) $N \times N$ square matrix shown in Fig. 1(a) is used to mimic the transport behavior. It is assumed there are two types of components with different conductive properties in the system. One is the FM metallic component (gray) due to the DE, the other is the PM component (white) due to the disorder scattering. A quantity f, defined as $f =$ (number of FM lattices)/(number of total lattices), is used to represent the fraction of FM metallic sites. At each site in this network, either a metallic or insulating resistance is located randomly and the total fraction of metallic component is f $(0 \leqslant f \leqslant 1)$. Obviously, f is equal to 1 at extreme low T due to the complete ferromagnetism and equal to 0 at high T due to the complete paramagnetism. For the intermediate temperature range, f is between 1 and 0, representing the coexistence of FM and PM states. This means the metallic fraction f varies with T. It should be noticed that f must decrease with the increasing T and should change rapidly near T_c [5]. So the function of the T-dependent f is similar to that of the magnetization measured in the system because f is proportional to the volume fraction of FM domains. As a matter of fact, f is the function of not only T but also H, which will be discussed later. For simplification, the function

$$f = \frac{1}{1 + B\exp[A(T - T_c + T_{\mathrm{MI}}^0 - T_{\mathrm{MI}}^H)]},$$

similar to the Fermi distribution function, is used to describe the T- and H-dependent f, where T_{MI}^0 and T_{MI}^H are the MIT temperature without and with H, respectively. A and B are the constants only depending on the material, and are set to be 0.01 and 1.22 in our simulation, respectively.

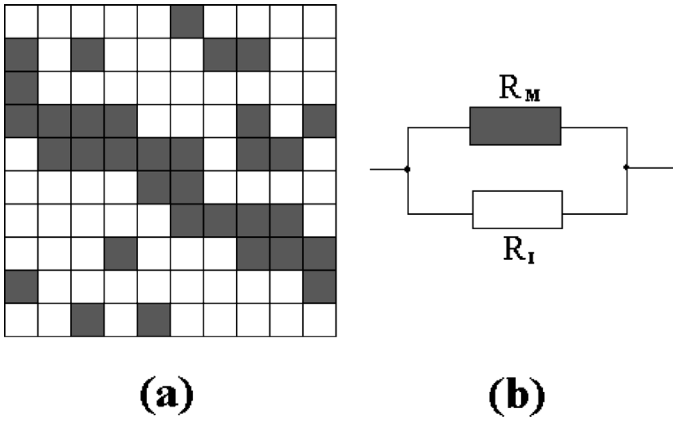

Fig. 1. (a) Schematic representation of the mixed-phase state of the FM metallic (gray) and PM insulating (white) domains. (b) Two-resistances model for calculating the effective resistance R from the parallel connection of metallic R_{M} and insulating R_{I} resistances.

We assume that the system is divided into two parts, as sketched in Fig. 1(b), being ferromagnetic metallic region with the resistance $R_{\mathrm{M}}(T)$ and the paramagnetic insulating region with the resistance $R_{\mathrm{I}}(T)$. The total effective resistance $R(T)$ is determined by the parallel connection of $R_{\mathrm{M}}(T)$ and $R_{\mathrm{I}}(T)$. Naturally, at low T, the current can flow only through the metallic paths due to the large f. Thus $R(T)$ is mainly determined by $R_{\mathrm{M}}(T)$. At high T, $R(T)$ is mainly determined by $R_{\mathrm{I}}(T)$ due to the small f. In the intermediate temperature range, the value of $R(T)$ is attributed to both $R_{\mathrm{M}}(T)$ and $R_{\mathrm{I}}(T)$. To calculate the resistance $R_{\mathrm{M}}(T)$ and $R_{\mathrm{I}}(T)$, we assume $\rho_m(T)$ and $\rho_i(T)$ are the resistivities for each FM site and each PM site, as the forms of $\rho_m(T) = \rho_{m0} + \rho_{m1}T^2 + \rho_{m2}T^{4.5}$ and $\rho_i(T) = \rho_{i0}\exp[E_0/(k_{\mathrm{B}}T)]$, respectively. In the FM metallic state, ρ_{m0} is the residual resistivity at $T \sim 0$ K; the T^2 term indicates the electron scattering [15] with the coefficient ρ_{m1}; the $T^{4.5}$ term denotes the magnon scattering involving the phonon scattering [16] with the coefficient ρ_{m2}. In the PM insulating state, a purely activated law for the semiconductor or insulator is used to express the T-dependent resistivity, which is described by the $\exp[E_0/(k_{\mathrm{B}}T)]$ term multiplied by the high-T residual resistivity ρ_{i0} [2,17], where the parameter E_0 is the activation energy and the symbol k_{B} represents the Boltzmann constant. The values of these parameters $(\rho_{m0}, \rho_{m1}, \rho_{m2})$ and $(\rho_{i0}, E_0/k_{\mathrm{B}})$ can be fitted from the experimental data in the low-T and high-T experimental data, respectively.

Breadth-first search [18] is a traversal through a graph that touches all of the nodes reachable from a particular source node. A breadth-first traversal (BFT) visits nodes that are closer to the source before visiting nodes that are further away. The distance is defined as the number of edges in the shortest path from the source node. This algorithm, which explores all nodes adjacent to the current node before moving on, can be used to compute the shortest path from the source to all reachable nodes and the shortest-path distances. When properly implemented, all nodes in a given connected component are explored. By using the BFT algorithm, the path lengths of the metallic and insulating domains are found. Then the resistances $R_{\mathrm{M}}(T)$ and $R_{\mathrm{I}}(T)$ are calculated, respectively. Finally, according to the size of the sample and the effective resistance $R(T)$, the effective resistivity ρ can be obtained. It is noticeable that this method is much convenient than the traditional way by solving the Kirchoff equations for the resistor network, as reported in the early literature [19–21].

3. Results and discussion

To explain the conductive behavior of the manganite LTMO, here we present our experimental data for the sample of LTMO in the temperature range from 5 K to 300 K, which has been published somewhere else [3]. As we will see later, the experimental results show the MIT behavior accompanied with a FM to PM transition, which is confirmed by the study on the T-dependent electron spin resonance spectra.

Based on the model and method mentioned above, the simulated resistivity vs. temperature (ρ–T) curve is obtained on 100×100 clusters without H on warming, as presented in Fig. 2. The corresponding experimental data (open triangles) are also given in this figure. The simulated curve (solid line) shows a good agreement with the experiment data, exhibiting the change from low-T behavior of $d\rho/dT > 0$ to high-T behavior of $d\rho/dT < 0$ with a FM to PM transition. The MIT temperature T_{MI} is about 165 K, lower than $T_c \sim 201$ K of the sample. The most striking aspect is that the residual resistivity ρ_{m0} is substantial even at very low T, suggesting that the metallic conduction path is irregular due to the small amount of PM component embedded in the FM domains. Moreover, the inset of Fig. 2 shows the results of the ρ–T relation obtained on 100×100 (solid line) and 200×200 (full circles) matrices, respectively, indicating that the 100×100 matrix is large enough to mimic the conductive behavior. Hence, only a 100×100 network is used in the latter simulation. It can be seen that the model not only results in the MIT, but also yields quantitative fits to the experimental data over the whole studied temperature range.

To further understand the coexistence of the phases and the percolative conductive behavior from the phenomenological view, a simulated transition process of the FM phase to PM phase without H is illustrated in Fig. 3 on a 100×100 matrix. In the program, the number of FM squares is determined by the T-dependent f. The position of the FM square on the 100×100 network is random. With the increase of T, metallic squares are randomly selected to be converted into insulating squares. The small dark squares represent the FM metallic sites and the white ones denote the PM insulating areas. The arrows indicate a warming process, i.e., the increase of the temperature. As shown in Fig. 3, the system undergoes a transition from a FM state with few PM domains at low T to a PM state with few FM domains at high T, showing the mixed-phase characteristics.

Now consider the influence of H on the resistivity of LTMO. The experimental data (open circles) and the consistent simulated result (solid line) are given in Fig. 4. Distinctly, there is a remarkable reduction in resistivity due to the alignment of the magnetizations of FM domains after applying H. Although the

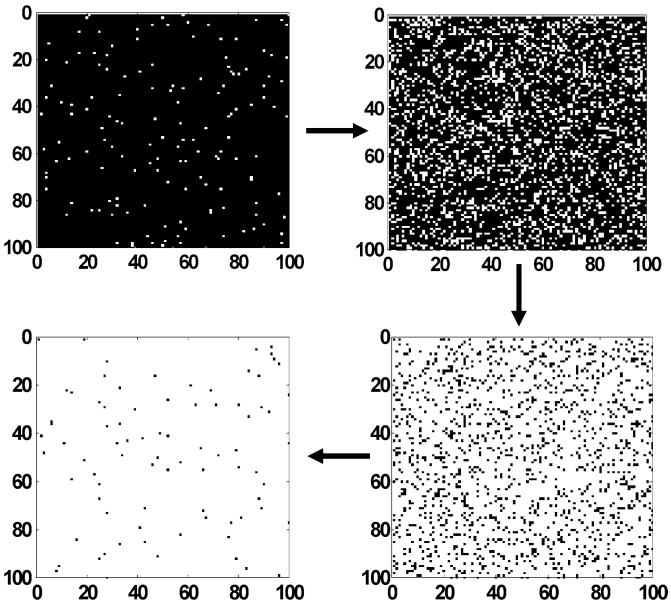

Fig. 3. Simulated process of the FM (black) to PM (white) transition from the low temperature to the high temperature in the mixed-phase description on 100×100 clusters. The arrows indicate the warming process.

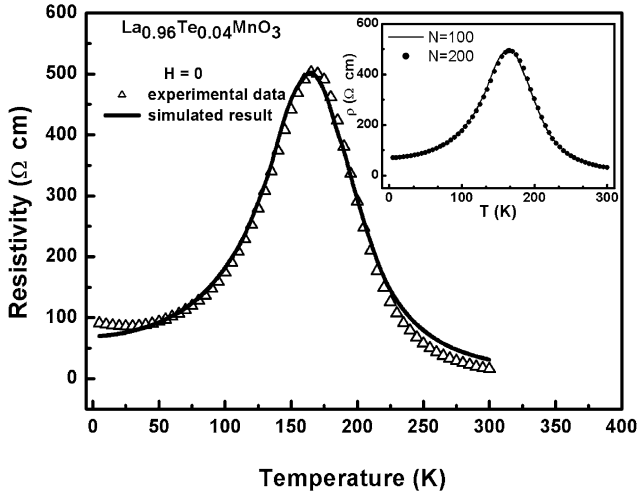

Fig. 2. Simulated ρ–T curve (solid line) of LTMO without H on a 100×100 matrix compared with the experimental data (open triangles). The inset is the results of the resistivities on 100×100 (solid line) and 200×200 (full circles) clusters, respectively.

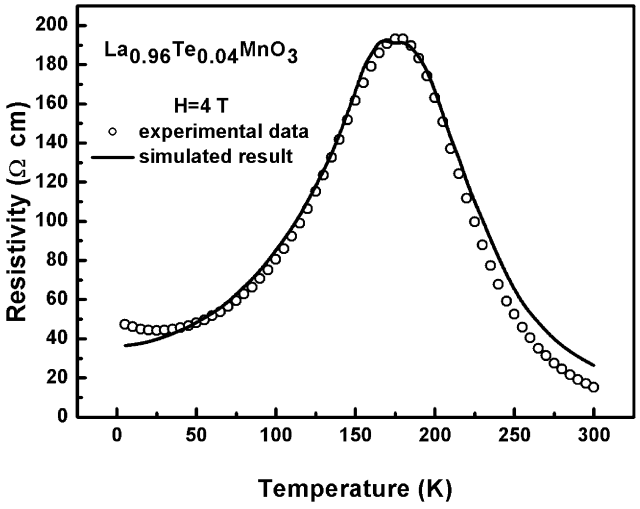

Fig. 4. Simulated result (solid line) and the corresponding experimental data (open circles) of the resistivities with H for LTMO.

Table 1
Parameters used in simulation for LTMO without and with H, respectively

H (T)	ρ_{m0} (Ω cm)	ρ_{m1} (Ω cm K^{-2})	ρ_{m2} (Ω cm K^{-4})	ρ_{i0} (Ω cm)	E_0/k_B (K)
0	58.8	0.0045	1.5×10^{-8}	0.48	1180
4	31.7	0.0028	2.3×10^{-10}	0.48	1110

MIT still exists with H, it can be seen that H slightly shifts the MIT temperature to a higher $T_{MI} \sim 175$ K. For the simulated result with H, the parameters are modified compared with those without H. The corresponding parameters used are listed in Table 1 for the zero and nonzero magnetic fields, showing some changes in the values of these parameters after applying H. First, the low-T residual resistivity ρ_{m0}, the electron–electron scattering coefficient ρ_{m1} and the magnon scattering coefficient ρ_{m2} are smaller than those without H. And this can be understood for the reason that H reduces the spin scattering in conduction carriers by driving the local orientation of magnetization aligned [6]. It should be pointed out that the coefficient ρ_{m2} decreases by two orders of magnitude, showing the magnetic field can suppress the magnetic scattering significantly. Second, the value of E_0/k_B is lowered, indicating that H can induce the reduction of the activation energy. Finally, the high-T residual resistivity ρ_{i0} remains unchanged. This is also reasonable because H may not reduce the resistivity of the PM components at very high T.

Furthermore, after applying H, the random spin disorder especially around T_c can be removed partially, causing a fraction of insulating regions to be converted into metallic regions [14]. This means H will increase the FM fraction f. In the random network model, it can be considered that the value of f is increased by a concomitant small amount with H. Naturally, the FM metallic fraction f is the function of not only T but also H. In order to show the influence of the H-dependent f on the resistivity clearly, the ρ–T curves in the external magnetic field are plotted in Fig. 5. The solid line is the pertinent calculated result extracted form Fig. 4, considering f is the function of T and H, i.e., $\partial f/\partial T \neq 0$ and $\partial f/\partial H \neq 0$. But the dotted line is obtained by ignoring the effect of H on the f, only regarding f is the function of T, i.e., $\partial f/\partial T \neq 0$ and $\partial f/\partial H = 0$. Obviously, the resistivity excluding the H-induced effect is larger than that including the influence of H, especially around MIT. So H can increase the FM fraction f in the percolative region and then decrease the value of the resistivity peak. Consequently, all those results indicate our simulation results agree with the experimental data and the changes in the values of the parameters also reflect the physical origin of the conductive behaviors.

According to our experimental results, the magnetoresistance (MR), defined as $\mathrm{MR} = [\rho(H) - \rho(0)]/\rho(H)$, where $\rho(0)$ and $\rho(H)$ are the resistivities under the zero and nonzero magnetic fields, respectively, is plotted in Fig. 6 (open circles). The maximum value of MR is about -174%, showing a pronounced negative MR at $T \sim 160$ K and displaying a CMR effect. The solid line is the calculated result from simulation. It is noticeable that those two MR curves almost overlap, indicating an excellent agreement between the experimental data and the simulated results.

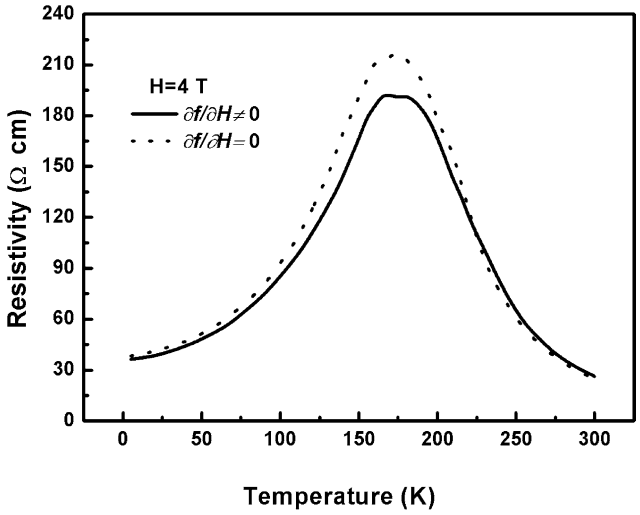

Fig. 5. Simulated ρ–T curves under the external magnetic fields with (solid line) and without (dotted line) the consideration of the H-induced effect on the FM metallic fraction f.

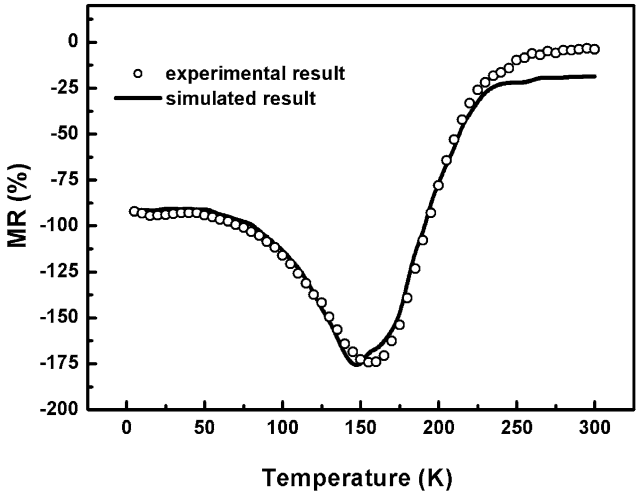

Fig. 6. The T-dependent curves of MR. The open circles are the experimental data and the solid line is the calculated result obtained by the previous simulated results.

In addition, Zhang et al. [22] have observed the MIT process using a low-T magnetic force microscope in $La_{0.33}Pr_{0.34}Ca_{0.33}MnO_3$, and found out that the MIT temperature T_{p1} on cooling is lower than the MIT temperature T_{p2} on warming. The results show a local magnetic hysteresis and indicate magnetic inhomogeneity. It suggests that the PM components still exist in the FM region at the temperatures lower than T_{p1} on cooling and the FM clusters are still embedded in PM state at the temperatures higher than T_{p2} on warming. If it is also correct for LTMO, we can deduce that the FM fraction f on cooling is slightly smaller than that on warming at a fixed temperature, especially in the intermediate temperature range. Based on the above assumption, we investigated the resistivity characteristics in a thermal cycle, as shown in Fig. 7. The dark lines are the previous simulated results on warming extracted from

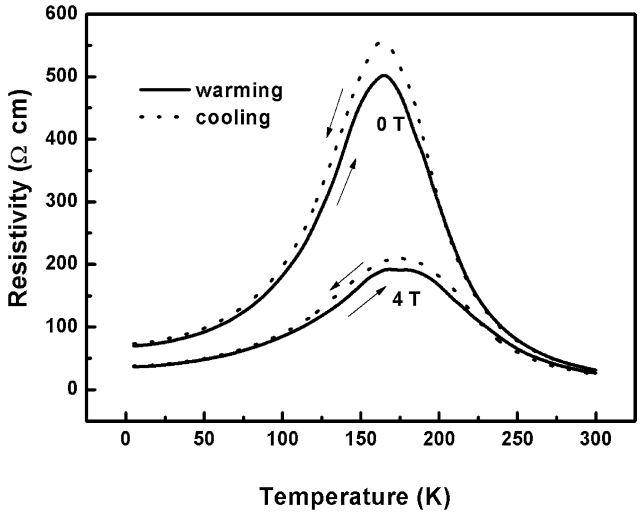

Fig. 7. Simulated thermal hysteresis of the resistivities in a temperature cycle in the zero and nonzero magnetic fields. The solid lines represent the simulated results on warming and the dotted lines indicate the simulated results obtained on cooling.

Fig. 2 and Fig. 4, respectively, and the dotted lines are the corresponding simulated results on cooling. It is worthy of note that the ρ–T curves obtained in the cooling process have different shapes compared to the results in the warming process, showing a thermal hysteresis resistivity phenomenon in the warming and cooling cycle in our model. This prediction is consistent with many experimental results [23,24].

4. Conclusion

In summary, based on the phase-separated framework, we have studied the T-dependent resistivity of $La_{0.96}Te_{0.04}MnO_3$ using the random network model. The breadth-first traversal algorithm is introduced to describe the transport problem and is found to be a valid algorithm by our current work presented in this Letter. By simulating the transport process in LTMO and obtaining the quantitative agreement with the experimental data, we have obtained the empirical formulas for T-dependent FM metallic and PM insulating resistivity, which had never been gained before in the theoretical simulation. Furthermore, a simulated transition process is illustrated to describe the mixed-phase transition in a warming process. We find that H has a significant influence on the conductive behavior of the mixed-phase manganite by suppressing the scatterings of the FM domains, reducing the activation energy of PM domains, and slightly increasing the FM metallic fraction. Those H-induced effects result in a remarkable reduction in resistivity, presenting a prominent negative CMR phenomenon. Under an assumption of a thermal hysteresis in magnetization, we predict that there is a similar thermal hysteresis phenomenon of the resistivity in the warming and cooling cycle for LTMO. All those results further verify that phase separation indeed lies in LTMO material and suggests that the intrinsic inhomogeneity plays a crucial role in the electrical conductivity.

Acknowledgements

We would like to thank Dr. Guo-tai Tan and Dr. Peng Han for their helpful discussions. This work is supported by a grant from the National Natural Science Foundation of China.

References

[1] M.R. Ibarra, J.M. De Teresa, J. Magn. Magn. Mater. 177 (1998) 846.
[2] S.L. Yuan, et al., Appl. Phys. Lett. 77 (2000) 4398.
[3] G.T. Tan, et al., Phys. Rev. B 68 (2003) 014426.
[4] M. Uehara, S. Nori, C.H. Chen, S.W. Cheong, Nature 399 (1999) 560.
[5] M. Mayr, et al., Phys. Rev. Lett. 86 (2001) 135.
[6] Y. Tomioka, et al., Phys. Rev. B 53 (1996) R1689.
[7] C. Zener, Phys. Rev. 82 (1951) 403.
[8] A.J. Millis, Nature 392 (1998) 147.
[9] R.M. Kusters, et al., Physica B 155 (1989) 362.
[10] S. Zhang, J. Appl. Phys. 79 (1996) 4542.
[11] R. Maezono, S. Ishihara, N. Nagaosa, Phys. Rev. B 58 (1998) 11583.
[12] A.J. Millis, B.I. Shraiman, R. Mueller, Phys. Rev. Lett. 77 (1996) 175.
[13] L.M. Rodriguez-Martinez, J.P. Attfield, Phys. Rev. B 54 (1996) R15622.
[14] M. Fäth, et al., Science 285 (1999) 1540.
[15] A.H. Thompson, Phys. Rev. Lett. 35 (1975) 1786.
[16] K. Kubo, N. Ohata, J. Phys. Soc. Jpn. 33 (1972) 21.
[17] A.K. Pradhan, Y. Feng, B.K. Roul, D.R. Sahu, Appl. Phys. Lett. 79 (2001) 506.
[18] S. Skiena, Implementing Discrete Mathematics: Combinatorics and Graph Theory with MATHEMATICA, Addison–Wesley, Reading, MA, 1990.
[19] S. Kirkpatrick, Rev. Mod. Phys. 45 (1973) 574.
[20] Z.Y. Li, S.L. Yuan, G. Peng, C.Q. Tang, Chin. Phys. Lett. 18 (2001) 1392.
[21] A. Moreo, J. Electron Spectrosc. Related Phenomena 117 (2001) 251.
[22] L. Zhang, et al., Science 298 (2002) 805.
[23] Y. Moritomo, H. Kuwahara, Y. Tomioka, Y. Tokura, Phys. Rev. B 55 (1997) 7549.
[24] H.Y. Hwang, et al., Phys. Rev. Lett. 75 (1995) 914.